Journal of Structural Geology 32 (2010) 59–69

Contents lists available at ScienceDirect

Journal of Structural Geology

journal homepage: www.elsevier.com/locate/jsg

Grain size distribution and microstructures of experimentally sheared granitoid gouge at coseismic slip rates – Criteria to distinguish seismic and aseismic faults?

Holger Stünitz [a,*], Nynke Keulen [b,d], Takehiro Hirose [c], Renée Heilbronner [b]

[a] Department of Geology, University of Tromsø, Dramsveien 201, 9037 Tromsø, Norway
[b] Dept. of Environmental Geosciences, Basel University, Bernoullistr. 32, 4056 Basel, Switzerland
[c] Kochi Institute for Core Sample Research, JAMSTEC, Kochi, Japan
[d] Geological Survey of Denmark and Greenland, Øster Voldgade 10, 1350 Copenhagen K, Denmark

ARTICLE INFO

Article history:
Received 9 December 2008
Received in revised form
1 July 2009
Accepted 4 August 2009
Available online 11 August 2009

Keywords:
Cataclasite
Rock deformation
Microstructures
Seismic deformation
Grain size

ABSTRACT

Microstructures and grain size distribution from high velocity friction experiments are compared with those of slow deformation experiments of Keulen et al. (2007, 2008) for the same material (Verzasca granitoid). The mechanical behavior of granitoid gouge in fast velocity friction experiments at slip rates of 0.65 and 1.28 m/s and normal stresses of 0.4–0.9 MPa is characterized by slip weakening in a typical exponential friction coefficient vs displacement relationship. The grain size distributions yield similar D-values (slope of frequency versus grain size curve = 2.2–2.3) as those of slow deformation experiments (D = 2.0–2.3) for grain sizes larger than 1 μm. These values are independent of the total displacement above a shear strain of about $\gamma = 20$. The D-values are also independent of the displacement rates in the range of ~1 μm/s to ~1.3 m/s and do not vary in the normal stress range between 0.5 MPa and 500 MPa. With increasing displacement, grain shapes evolve towards more rounded and less serrated grains. While the grain size distribution remains constant, the progressive grain shape evolution suggests that grain comminution takes place by attrition at clast boundaries. Attrition produces a range of very small grain sizes by crushing with a $D_{<}$-value = 1. The results of the study demonstrate that most cataclastic and gouge fault zones may have resulted from seismic deformation but the distinction of seismic and aseismic deformation cannot be made on the basis of grain size distribution.

1. Introduction

Fault rocks, and especially fault rocks from seismic events, have received increasing attention over the past years. In the field, it is extremely difficult, if not impossible, to distinguish between seismic and aseismic fault rocks (Cowan, 1999, Sibson, 1989). So far, the occurrence of pseudotachylites appears to be the main reliable criterion for the identification of seismic slip in natural fault rocks (McKenzie and Brune, 1972, Sibson, 1975, Spray, 1992, 1995, 1997). Another criterion is the occurrence of clay-clast-aggregates in clay-rich gouges (Boutareaud et al. 2008). Alternatively, the direct association of fault zones with active faulting, e.g. in the San Andreas fault system or the Nojima fault of the Kobe earthquake may be used to infer that seismic slip has occurred in the fault rocks (Sammis et al., 1987, Wilson et al., 2003, Chester et al., 2005, Murata et al., 2001, Monzawa and Otsuki, 2003). These criteria apply to a small number of faults. For the large part of the natural inventory of fault rocks, which may be available for detailed analysis as potentially seismic zones, seismic slip rates cannot be inferred with certainty. If measurable properties, such as grain size, grain shape, etc. could be used to identify fast slip rates, a large number of natural faults from all geological periods and from many different tectonic settings would be available for studies of processes and mechanisms of the earthquake cycle.

One way of obtaining information about deformation processes in fault rocks is to perform experiments employing fast slip rates as these may simulate seismic slip rates (e.g. Spray, 1987, 1993, Tsutsumi and Shimamoto, 1997, Hirose and Shimamoto, 2003, 2005, Mizoguchi et al., 2007, Han et al., 2007a, b, Boutareaud et al., 2008). We have carried out fast slip experiments on granitoid fault gouge, because there is data of microstructures and grain size distributions of the same material from slow deformation experiments. The experiments at slow deformation rates have been carried out in a Griggs solid medium apparatus by cracking of solid samples of granitoid material followed by sliding of the fragments at high confining pressures and a range of temperatures (Keulen et al., 2007, 2008). The objectives of the present investigation are to

* Corresponding author. Fax: +47 77 64 56 00.
E-mail addresses: holger.stunitz@uit.no (H. Stünitz), hiroset@jamstec.go.jp (T. Hirose), renee.heilbronner@unibas.ch (R. Heilbronner).

0191-8141/$ – see front matter © 2009 Elsevier Ltd. All rights reserved.
doi:10.1016/j.jsg.2009.08.002

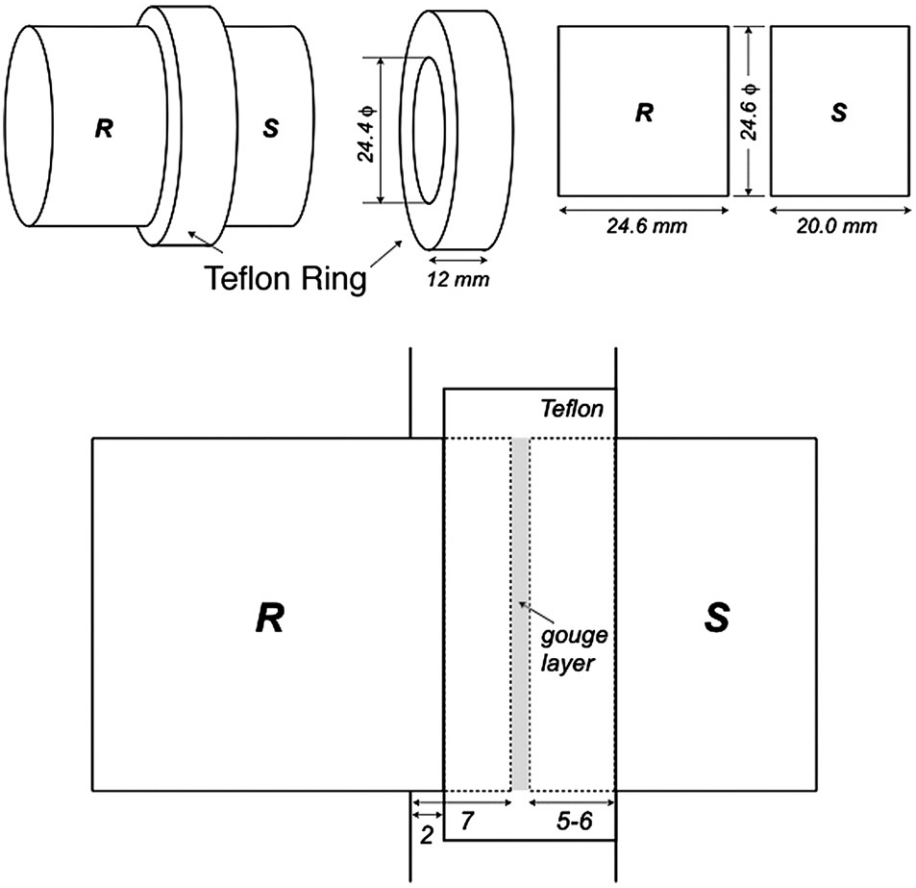

Fig. 1. Schematic view of the sample assembly in the fast rotary shear apparatus. R = rotation side of the assembly, S = stationary side of the assembly. Dimensions are given in mm.

study the evolution of the grain size distribution at different slip rates and at different amounts of total slip in order to obtain information about the comminution process, the dependence of sliding on the microstructures, and to potentially quantify the evolution of the grain size distribution for different rates of slip (seismic and aseismic) and for different total amounts of slip.

2. Experimental and analytical procedures

The fast slip experiments have been performed on crushed starting material from Verzasca gneiss in a high speed rotary testing apparatus (Shimamoto and Tsutsumi, 1994). The crushed material has been prepared from the same Verzasca granitoid gneiss material as the slow deformation experiments of Keulen et al. (2007, 2008). Verzasca gneiss is a fine-grained granitoid gneiss (grain size ~280 μm) with almost no secondary alteration minerals and a very weak planar and linear fabric. The location of the sample of the starting material is: Swiss coordinates 704.65/126.30; the composition is: 29% plagioclase, 27% K-feldspar, 35% quartz, 7% mica (mostly biotite).

The starting material has been prepared by pounding of the solid rock and large fragments (only once or a couple of times) and sieving the fine fragments after pounding. The larger fragments have been pounded and sieved again until the grain size of the starting material has been smaller than 500 μm. By this procedure, we attempt to produce fragmented material more typical of natural damage zones rather than cataclastic or gouge material which is typically produced in natural slip or process zones after extensive attrition and wear.

The starting material (1g) has been placed between roughened (ground flat using no. 80 SiC powder) cylinders of Verzasca gneiss (24.5–24.6 mm diameter; Fig. 1), resulting in about 1 mm thick layers of the crushed material. No water has been added but some water may be present as a result of adsorption from air humidity. A Teflon sleeve (Fig. 1) holds the crushed material in place during shearing but no confining pressure is applied. The sample is inserted into a high speed rotary shear apparatus (Tsutsumi & Shimamoto 1994) and deformed at different slip rates and different amounts of total displacement and normal stress (Table 1). The slip rate of the sample varies between 0 at the center and the maximum rate at the periphery. An "equivalent slip velocity" V_{eq} (termed "slip rate" in this text) is defined by obtaining the frictional work rate W_r on the slip surface area S assuming that the shear stress τ is constant over the slip surface and does not vary with velocity :

$$W_r = \tau \; V_{eq} \; S \qquad (1)$$

Table 1
Results of fast experiments performed on high speed rotary testing apparatus. Inferred temperature for all experiments 400 °C (see text).

Sample Number	Normal stress [MPa]	Slip rate [m s-1]	Steady state friction coefficient	Total displacement [m]	Average D-value of gouge
HVR 833	0.8–0.9	1.28	0.35–0.45	24	2.24
HVR 835	0.8–0.9	1.28	0.35–0.5	26	
HVR 836	0.8–0.9	0.65	0.57–0.7	20	2.26
HVR 840	0.8–0.9	1.28	0.35–0.5	36	
HVR 841	0.8–0.9	1.28	0.45–0.55	11	
HVR 842	0.4–0.5	1.27	0.45–0.65	39.5	2.26

(Shimamoto and Tsutsumi, 1994, Hirose and Shimamoto, 2005). In practice, the value of the equivalent slip velocity is approximately equal to the slip rate at the periphery divided by 1.5.

After the experiment, the crushed starting material is much finer in grain size and represents a fault gouge typical for extensive slip, attrition, and wear. A minor amount of shortening occurs during the experiment, partly by compaction of the gouge during the rotation, partly by small amounts of gouge moving between the cylinders and the Teflon sleeve. All experiments have been carried out at room temperature, but some shear heating of the samples has occurred. The sample temperature has not been measured, but gouge experiments of Boutareaud et al. (2008) were performed under the same slip rates and the same normal stress. Boutareaud et al. (2008) have measured peak temperatures around 400 °C, and we infer similar temperatures for our experiments. No melt has been detected in any of the samples.

After the experiments, the Teflon ring was removed using a C-clamp to hold the forcing blocks in place. The gouge was vacuum-impregnated with Laromin, a low viscosity epoxy. After impregnation, the samples were cut for thin sections parallel to the rotation axis, about 3–4 mm from the periphery of the cylinder.

The shape analysis of grains was carried out on SEM-BSE micrographs using the image analysis program "Image SXM" (Barrett, 2002, http://www.liv.ac.uk/~sdb/ImageSXM) and the fabric analysis programs "paror", "surfor" and "ishapes" (Panozzo, 1983, 1984, Heilbronner and Keulen, 2006, http://www.unibas.ch/earth/micro). Particles have been segmented automatically and, where necessary, manually. Two parameters are used to describe fragment shapes: (1) Aspect ratio, defined by the long and short axes of projected particles, and (2) Paris factor, which is derived from the difference between the length of the outline of a particle and the length of its convex envelope. A Paris factor of 0% represents particles with completely convex, uncorrugated surfaces, whereas higher Paris factors indicate more serrated boundaries and/or concave shapes. For more details of the analysis, see Heilbronner and Keulen (2006).

For the grain size analysis "Image SXM" is used, following the routine outlined in Keulen et al. (2007). The grain size is described by the radius, r, of the area-equivalent circle of the 2-dimensional cross sectional areas of the grains. The negative slope of the log(#)-log(r) plots yields the D-value. This value applies to the size distribution of 2-D grain areas. The fractal dimension of the size distribution of 3-D grains is obtained by adding the value of 1.00 to D.

3. Results

3.1. Mechanical data

A total of six samples were deformed (Table 1). As can be seen in Fig. 4, at the beginning of the slip, the friction coefficient is sometimes higher than 1.0. This is partially due to the effect of frictional resistance between Teflon sleeve and host rock, that is often around 0.1 MPa in shear stress (e.g., Mizoguchi et al., 2007). However this resistance reduces gradually to nearly zero at high slip rates, so we did not correct the effect of Teflon friction for the mechanical data.

Four samples, HVR 833, 835, 840, and 841, were deformed at a slip rate of 1.28 m/s and a normal stress of 0.8 to 0.9 MPa, but to different amounts of total displacement (Table 1, Fig. 2 a–d). These experiments show a good reproducibility and similar characteristics of mechanical behavior: The friction coefficient decreases after some displacement and reaches a lower (more or less) steady state mean value of $\mu = 0.4–0.5$ for most samples after 8–10 m (slip weakening distance D_c) of slip (Fig. 2 a–d). The slip weakening distance is in a similar range as that determined for other fast slip experiments on fault gouge (Mizoguchi et al., 2007, Brantut et al., 2008).

The slip weakening critically depends on slip velocity: Sample HVR 836 which was deformed at half the slip rate (0.65 m/s) only weakens to a friction coefficient of 0.6–0.7 (Fig. 2e), compared to 0.4–0.5 of the fast slip experiments at 1.28 m/s. Similar findings have already been described by Mizoguchi et al. (2007) and Tsutsumi and Shimamoto (1997). Our results are also in accord with those from slower friction experiments (e.g. Marone, 1998, and references therein).

On the other hand, the normal stress does not seem to affect the friction coefficient of the weakened stage of slip very much. The mean friction coefficient of experiment HVR 842 (Fig. 2f) is only slightly higher than that of the other samples at the same slip rate (Fig. 2a–d). The initial peak friction coefficient of sample HVR 842 is higher, possibly due to some initial compaction effects of the crushed rock under the lower normal stress.

All weakening parts of the curves show the typical exponential decay relationship of the friction coefficient with increasing slip distance (e.g., Hirose and Shimamoto, 2005, Mizoguchi et al., 2007). Minor variation in the mechanical data is attributed to the microstructural heterogeneity of the slip zones and their complex internal structure (see below).

3.2. Microstructures

In all of the deformed samples, there is a distinct layering of the gouge material (Fig. 3). The layers may be distinguished primarily on the basis of grain size (layer 3 always contains less fine grained material than layers 1 and 2), or on the basis of color (layer 1 is always darker than layer 2). The origin of the dark color (most obvious in layer 1) of the gouge is not entirely clear. At higher magnification, the layers can still be distinguished in SEM images by what appears to be dark "holes" or cavities between grains (Fig. 4a). In plane polarized light in the light microscope, very fine-grained dark particles and no porosity can be observed between fragments. Thus, these dark regions are not cavities or pores but consist of very small solid particles with a low atomic number contrast in the SEM. An identification of these particles has not been possible but their low atomic number suggests that these probably are carbon-rich breakdown products from the Teflon sleeve around the sample.

The thin sections were prepared close to the periphery of the samples, tangential to the cylinder, parallel to the rotation axis. They are assumed to represent the same shear strain rate throughout the area of analysis; any effect of the radial strain gradient from the periphery to the central axis is neglected.

In one sample, three layers are developed (layers 1, 2, 3; HVR 833, Fig. 3a), in others only two (layers 1 and 2; HVR 836 and 842, Fig. 3b,c). The boundary between layers can be sharp and planar (Fig. 3a), irregular (Fig. 3b), or convoluted (Fig. 3c). In some samples, there are repetitions of layers, especially where their boundary is convoluted. These structures indicate some non-laminar movement of the layers in the gouge, at least for part of the deformation.

In many cases, elongated fragments are aligned or are oriented at a low angle with the shear plane (Fig. 3). In layers of type 1, the main gouge layer, fragments have more rounded corners and smoother edges than in layers 2 and 3 (Fig. 3), suggesting that a higher amount of slip (with more attrition) has been accommodated in layers of type 1. Layer 3 in HVR 833 shows a considerably larger amount of coarse grains, indicating that very little, if any, displacement has been accommodated in this layer.

In HVR 836, a very thin (0.015–0.06 mm) dark layer of variable thickness (without any coarser fragments) is in direct contact with the solid cylinder (Figs. 3b, 4b). This thin layer shows some internal fabric consisting of bands of very fine grains (Fig. 4c). The bands have an internal S-geometry (in the sense of S-C-fabrics) consistent

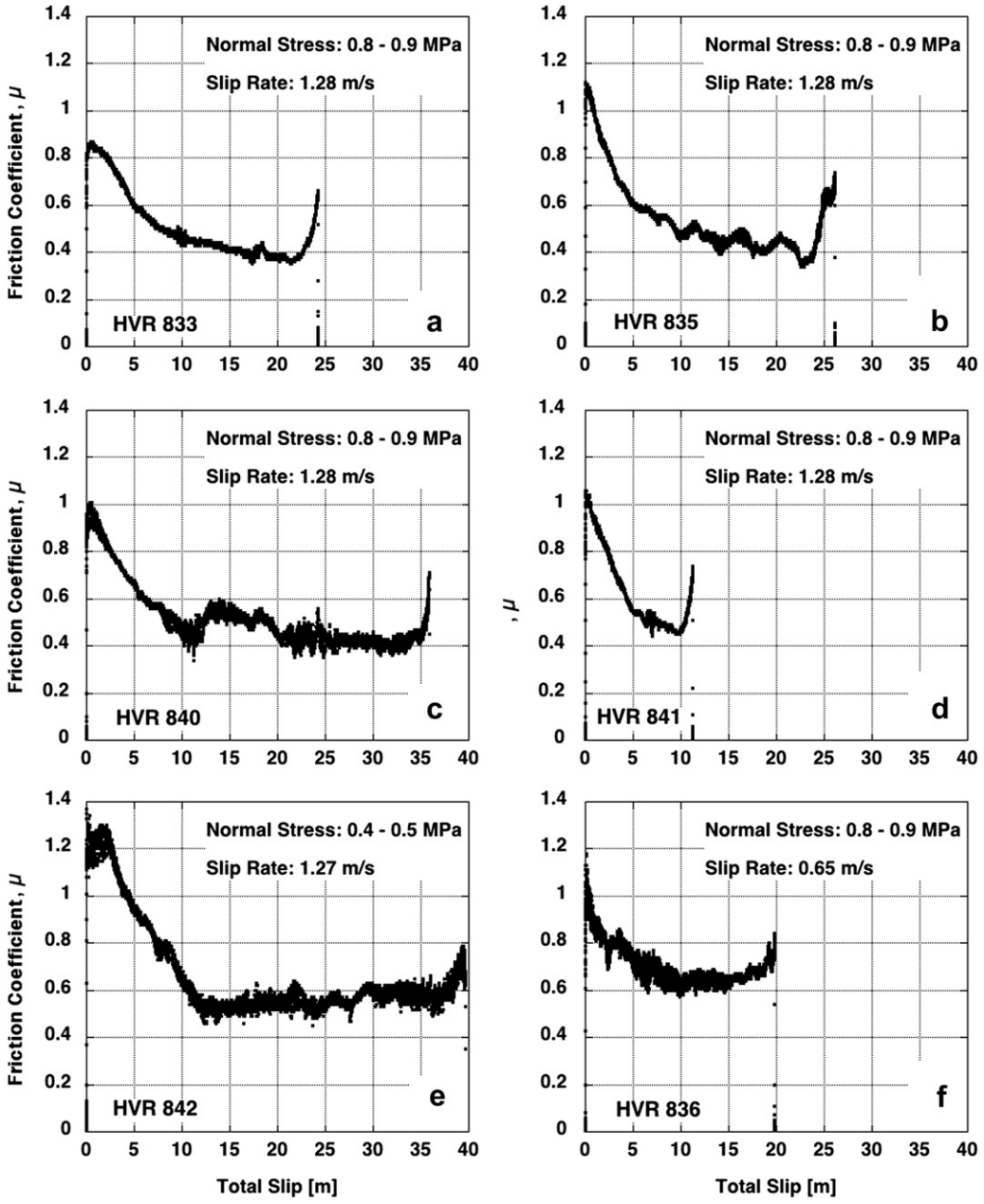

Fig. 2. Friction coefficient, μ, of the experiments versus the slip distance calculated for the "equivalent slip velocity". Weakening is similar in all experiments. a.) to d.) Experiments at 0.8–0.9 MPa normal stress, slip rate of 1.28 m/s, e.) Experiments at 0.4–0.5 MPa normal stress, slip rate of 1.27 m/s, f.) Experiment at 0.8–0.9 MPa normal stress, slip rate of 0.65 m/s.

with the applied shear sense (Fig. 4b,c). In the same thin layer, there is a gradient in grain size with the coarser sizes at the lower solid cylinder interface to very fine grains at the interface with the main gouge layer (layer 1, Fig. 4b). The grain size gradient is interpreted to result from a greater amount of slip in the very fine-grained parts between the main gouge layer and the solid rock.

Some clasts in the gouge show local attrition or spalling at their margins (Fig. 4d). The grain size in these attrition zones is generally smaller than in the normal gouge. The grain size in the normal gouge can be very small, the smallest particles detected are below 100 nm (Fig. 4e).

3.3. Grain size distribution

The grain size distribution (GSD) is represented in log grain size versus log frequency diagrams (Fig. 5a). The D-value is determined from the slope of the best fit to the grain size vs. frequency relationship (Fig. 5a; Sammis et al., 1986, Heilbronner & Keulen, 2006, Keulen et al., 2007). There are two slopes, $D_>$ for grain sizes larger than r_k, and $D_<$ for grain sizes smaller than r_k (Fig. 5a). The value for r_k denotes the change in slope of the grain size vs. frequency relationship and has a value between 1.1. and 1.3 μm for the samples of this study. The origin of the slope change is most likely related to the grinding limit (An & Sammis, 1994, Keulen et al., 2007), a critical grain size above and below which the comminution mechanism of the minerals are different. The observed $D_>$-values, $D_<$ -values, and r_k values are very similar to those found in the fine grained material of slow deformation experiments of Keulen et al. (2007). In the slow deformation experiments, the D-values of quartz and feldspar were determined separately, whereas for the fast slip experiments only a single value was determined for feldspar and quartz. An average value between

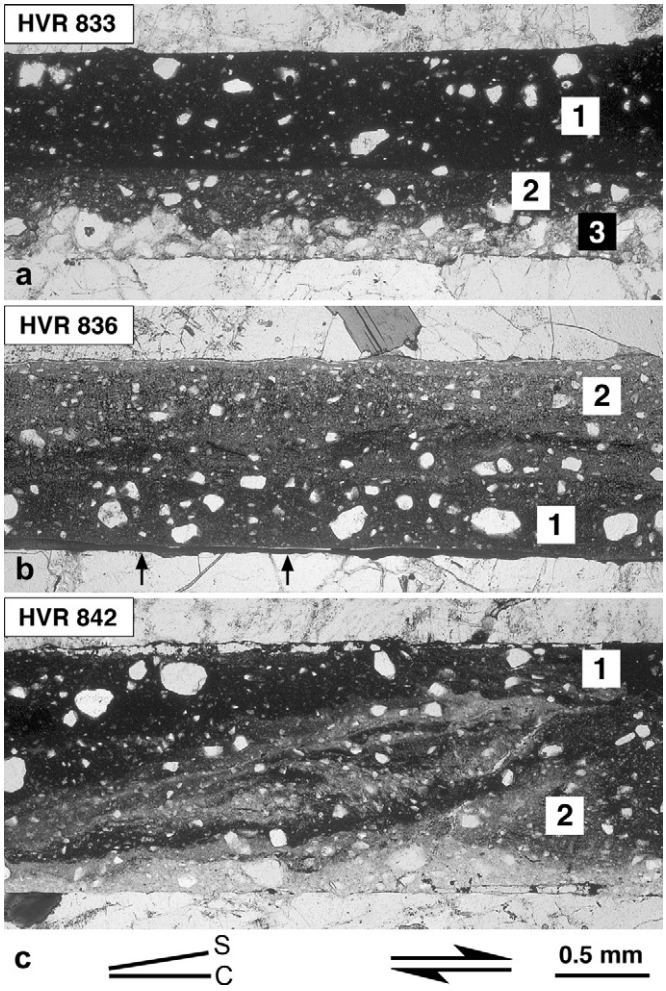

Fig. 3. Light micrographs of the deformed samples selected for microstructural and grain size analysis (plane polarized light). Light material at top and bottom are the solid cylinders between which the crushed material (darker) has been deformed. Sense of slip and scale apply to all. Numbers refer to the layers for which the shape and grain size analysis has been carried out (see text). a.) HVR 833, b.) HVR 836. Arrows point to slip zone at the bottom of the gouge zone directly in contact with the solid cylinder. c.) HVR 842. S-C-geometry of the slip zone is indicated.

feldspar and quartz is used for slow slip samples to compare them with fast slip ones.

The D-values of layer 1 and 3 in sample HVR 833 differ (Fig. 5a). The values of 2.23 (layer 1) and 1.54 (layer 3) correspond to values for gouge and cracked material, respectively, measured in slow deformation experiments of the same starting material (Keulen et al., 2007). "Cracked" denotes fractured grains, where the original geometric relationship of the fragments can still be recognized (i.e. very little displacement between fragments), whereas "gouge" refers to material where the fragments are rounded and displaced with respect to each other. Layer 3 corresponds to cracked grains of the slow deformation experiments, whereas layers 1 and 2 correspond to the gouge of the slow deformation experiments (Keulen et al., 2007). The $D_{>}$-values observed in fast slip experiments are the same as those of cracked and gouge material of slow deformation experiments (cf. Keulen et al., 2007) and allow the distinction of cracked material (layer 3) and gouge material (layer 1).

For the loose starting material a single D-value of 1.2 is measured (Fig. 5b), which is lower than the D-value of layer 3 ($D_{>} = 1.54$). The reason for the lower D-value may be the absence of compaction of layer 3. During the experiment., the compaction is likely to cause further comminution of the grains, resulting in an increased D-value of 1.54.

The D-values of layer 1 and 2 in sample HVR 833 are indistinguishable (Fig. 5b). Thus, the difference in color between these layers is due to the black color of the fine particles only and not to differences in GSD. The same $D_{>}$-values of = 2.2–2.3 are also found in the corresponding layers in samples HVR 836 and HVR 842 (Fig. 5b), which have been deformed at a slower slip rate (HVR 836, Fig. 2e) and at a lower normal stress (HVR 842, Fig. 2f). Thus, all D-values observed in fast slip experiments correspond to those of cracked and gouge material of slower deformation experiments and are independent of normal stress and slip rate within the range of tested parameters.

3.4. Shape analysis of gouge

Three of the deformed samples have been selected for detailed quantitative microstructure analysis (HVR 833, 836, and 842). The three layers of sample HVR 833 have been analyzed individually as they represent examples of different amounts of total slip (concluded from the grain size analysis), from layer 3 (cracked material - very little slip) to layer 1 (gouge material - large amount of slip).

A plot of the Paris factor (Heilbronner & Keulen, 2006) which is a measure of convex and concave particle shapes (low Paris factor = convex shapes) versus the aspect ratio shows a decrease in the scatter of the data from layer 3 to layer 1 (Fig. 6a–c). The values converge towards low Paris factors and low aspect ratios in the layer 1, where a large amount of the total slip has taken place (Fig. 6a). The average values of all data from each layer show this trend clearly (Fig. 6d). The starting material is also included and indicates that for no or very little slip or compaction, there is mainly a reduction in the Paris factor (difference between the Paris factor of starting material and layer 3). This reduction represents a rounding of fragment surfaces from angular and serrated to more convex shapes. This shape change can be explained best by spalling and abrasion of fragments in the deforming matrix of gouge. For increasing slip, the aspect ratio decreases, too, indicating that elongate particles are preferentially affected by the fragmentation and spalling. The result of continued fragmentations and spalling are equant, progressively rounded grains (Fig. 6).

4. Discussion

4.1. Experiments

The results of the GSD are quite clear: All samples show the same values for $D_{<}$, $D_{>}$, and r_k for layers 1 ,2 and 3, independent of slip rates and normal stresses, indicating that these parameters do not affect the grain comminution. The GSD's of the fast slip rate experiments can be compared to those of the slow deformation experiments performed on the same granitoid sample material (Fig. 7a,b), although total strains are very different, too. For the fast slip experiments, all minerals were analyzed together and represented by single D- and r_k-values (Table 1), whereas for the slow deformation experiments, quartz and feldspar in the granitoid gouge have been analysed individually (Table 2). We therefore compare the D-values of this study with an average D-value of quartz and feldspar for the slow deformation samples (Fig. 7a,b). The plot covers different slip rates over a range of 8–9 orders of magnitude. All $D_{>}$-values for slip rates of 1.28 m/s (fast slip experiments) and ~1 μm/s (slow deformation experiments of Keulen et al., 2007, 2008) lie between 2.0 and 2.35, so that there appears to be no systematic difference in D-values of fault gouge for these very different slip rates. The fact that the lowest $D_{>}$-values

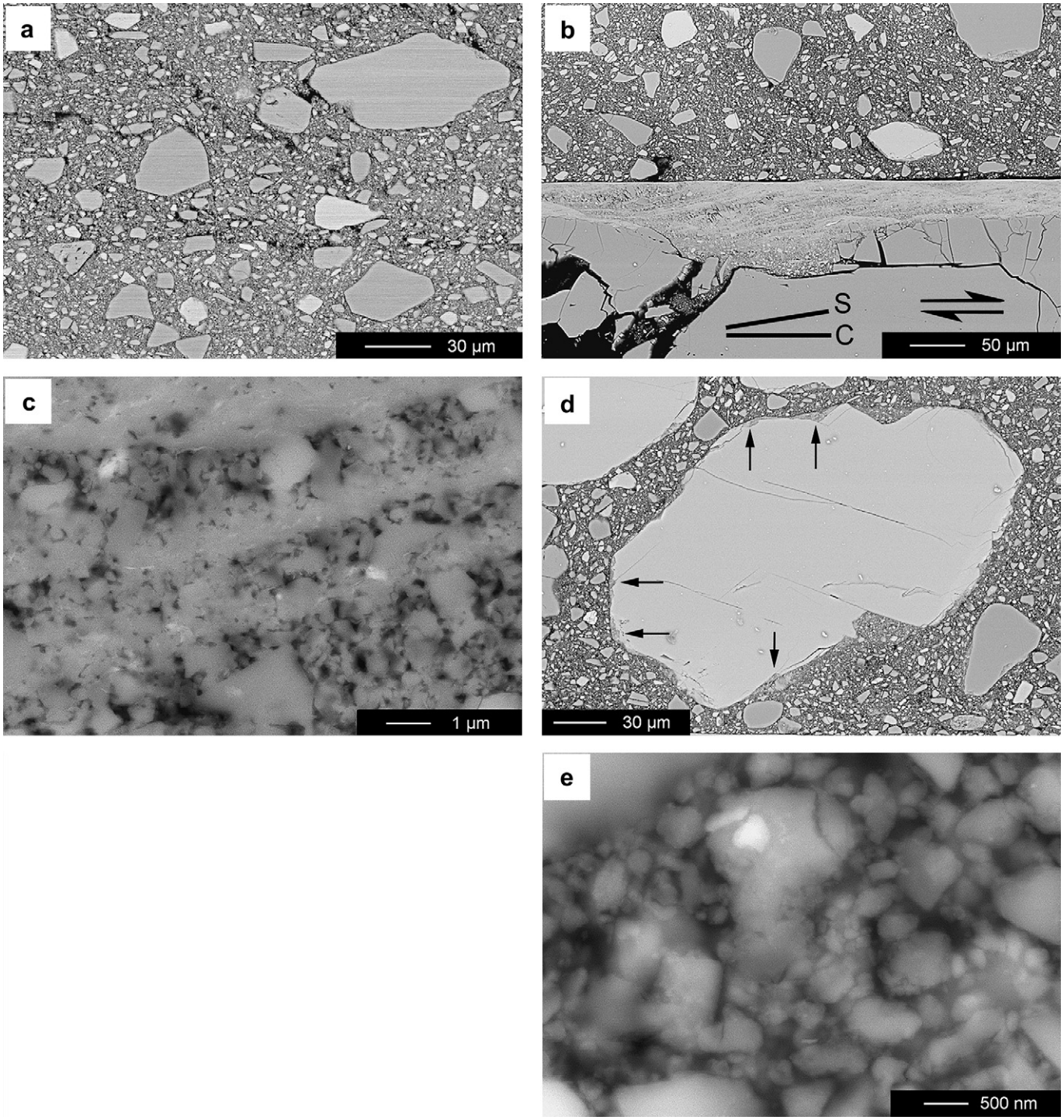

Fig. 4. SEM backscatter micrographs of the experimental fault gouge. a.) Section across the boundary between layer 1 and 2 in sample HVR 833 (Fig. 3a). The darker layer 1 (upper 2/3 of the image) can be distinguished from the middle layer 2 (lower 1/3 of image) because of dark material along some of the grain boundaries. b.) Detail of the finer grained slip zone at the contact between the gouge zone (layer 1) and the solid rock in sample HVR 836 (Fig. 3b). S-and C- geometry of slip zone is indicated. c.) Detail of the material in the fine grained slip zone of Fig. 4b showing bands of different grain sizes in the S-planes. d.) Boundary region of a clast where finer grained material forms at the clast surface by attrition. Sample HVR 836, layer 1. e.) Fine grained material in gouge, layer 1 in sample HVR 836.

are found at 500 °C may point to temperature effects, which may become important around or above 500 °C.

Cracked grains (= layer 3) in fast and slow experiments show the same D-values of 1.5–1.7 (Fig. 7b). The lower D-values for cracked material in slow deformation experiments correspond to those of layer 3 of fast slip experiments and are consistent with observations by Marone & Scholz (1989) who have found lower D-values for hydrostatically loaded and low shear strain samples. Cracked material from our experiments may be similar to the damage zones, whereas gouge material from our experiments may be similar to process or slip zones in natural faults.

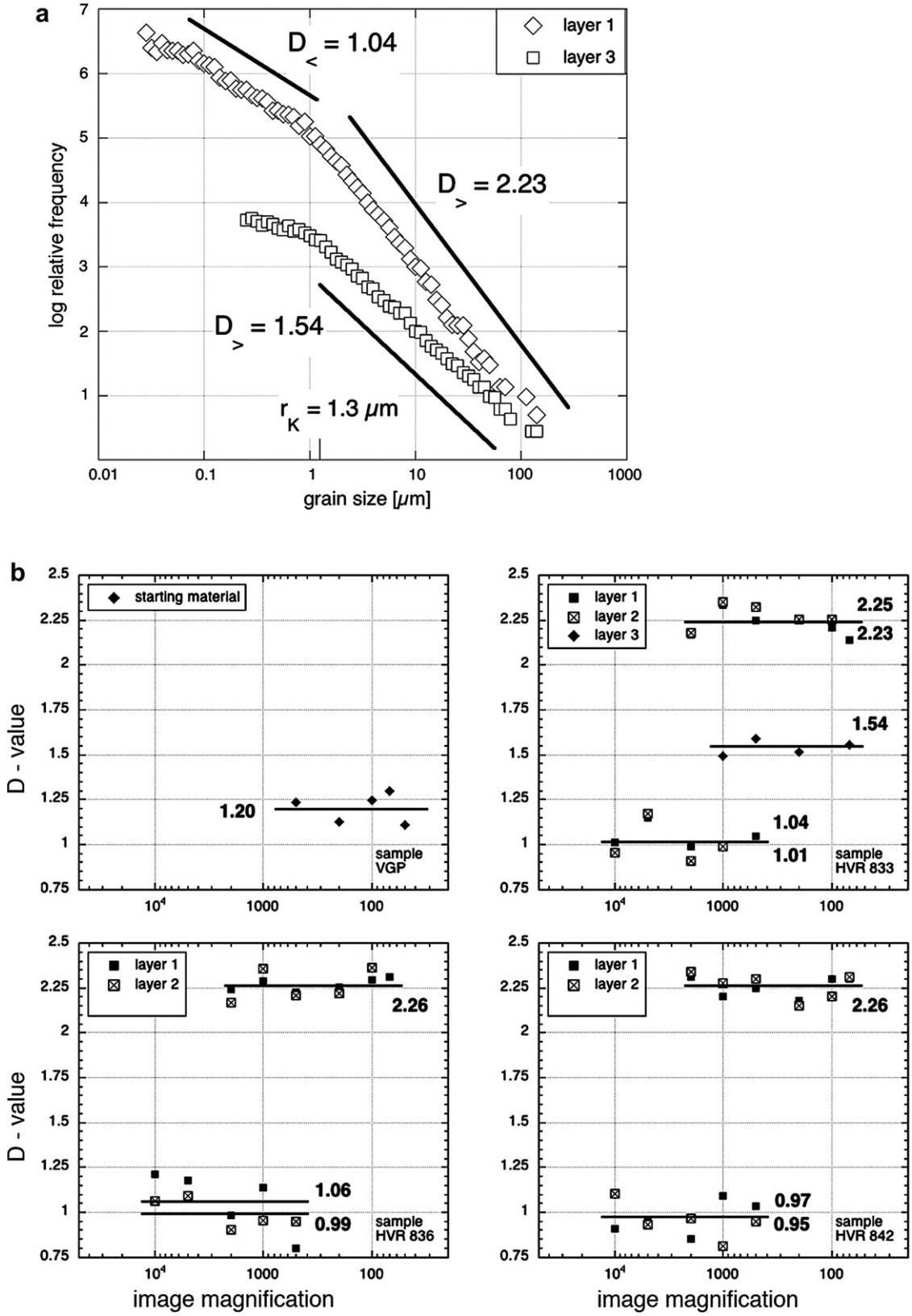

Fig. 5. (a) Grain size distribution for sample HVR 833 in a log - log plot of grain size versus frequency. The values r_k indicates the grain size value where slope of the grain size – frequency relationship changes in layer 1. The solid lines indicate the slopes for the fitted D-values. $D_>$ = D-value of grain size larger than r_k; $D_<$ = D-value of the material smaller than r_k; r_k = grain size-value where the change in slope occurs. (b) D-values of the the starting material and three of the deformed samples.

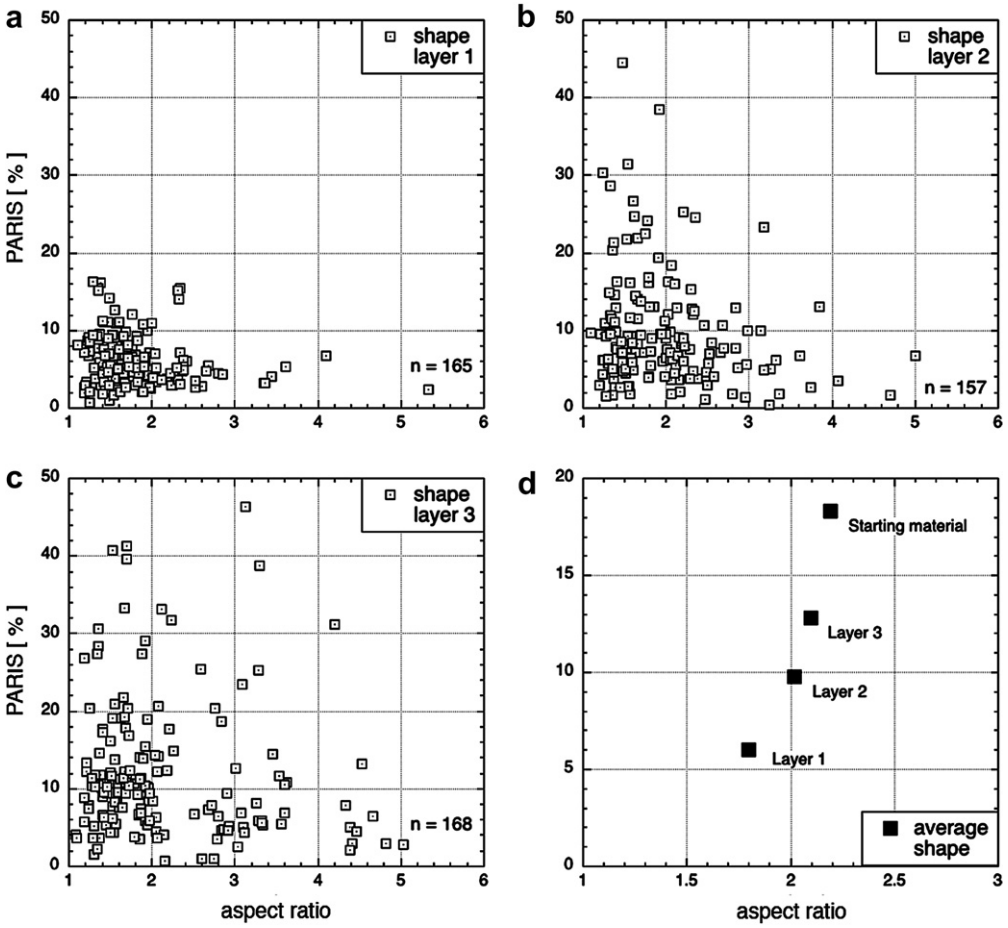

Fig. 6. Paris factor versus aspect ratio in the different layers of sample HVR 833. (a) Layer 1, (b) Layer 2, (c) Layer 3 at the bottom contact with the solid cylinder (see Fig. 3a). (d) Average values for the grain shapes from plots (a) to (c).

The normal stress in the slow deformation experiments is much higher (500 MPa) than in fast slip experiments as the former have been carried out in a solid medium Griggs-type apparatus. The same D-values in the fast slip experiments at low normal stress and in slow deformation experiments at high confining pressure indicate that there is no dependence of the D-value on pressure within the range of tested values (0.5–500 MPa). The confining pressure has been found to affect the D-value only at much higher confining pressures (1 GPa; Keulen et al., 2007) where mode II cracking is inferred as the dominant process during grain comminution (Hirth & Tullis, 1994).

It is interesting to note that the fast experiments at low normal stress and the slow experiments at high normal stress levels produce similar GSD's. One possible way of reconciling these findings is to compare the D-values in terms of the work done to the gouge. The energy involved derives both from normal or shear stress and from displacement or shear strain rate. An additional set of experiments is necessary to test the separate influence of stress and displacement rate.

Lower D-values ($D_{>} = 1.7–1.9$) have been observed for some of the very slow deformation experiments ($10^{-1}$to 10^{-2} μm s^{-1}) that lasted for several days or weeks (Keulen et al., 2008). These low D-values have been determined in the gouge of higher temperature experiments at 500 °C (Fig. 7a). The lower D-values are caused by grain growth processes, which compete with comminution at slow rates of deformation and temperatures above 300 °C (Keulen et al., 2008). It is interesting to note that the grain growth effect is only observed in gouge, not in the cracked material of slow deformation experiments (Fig. 7b) and not in layer 3 (equivalent of cracked grains) of the fast slip experiments. The reason for the absence of temperature effects in the cracked material in fast slip experiments seems to be that (1) the temperature prevails only for less than one minute, and (2) grain growth is not as effective if there are only a few very fine grains, which is the case in the cracked material as it has not been sliding (Keulen et al., 2008). The very fine grains disappear during the grain growth, presumably by dissolution (Keulen et al., 2008).

The same D-values in slow and fast deformation experiments have developed after very different amounts of total displacement. The maximum total slip in slow deformation experiments is on the order of a few mm (Keulen et al., 2007, 2008), whereas the total slip for the fast slip experiments varies between 10 and 37 m (Fig. 2). In order to compare these values, the total shear strain is used, because the thickness of the slip zones is quite different in slow deformation and fast slip experiments. The total shear strain in the slow deformation experiments varies substantially. The thickness of the individual displacement zones (cracks) varies between 10 μm and 1 mm. Given a large variation in displacement, the maximum shear strain values are on the order of $\gamma = 20–60$, whereas that of the fast slip experiments varies between $\gamma = 15'000$ and 33'000. Thus, taken together, the high and low speed experiments demonstrate that the GSD of the sliding gouge develops after $\gamma \sim 20$ and then remains approximately constant. Although the amounts of displacement recorded in slow deformation experiments are

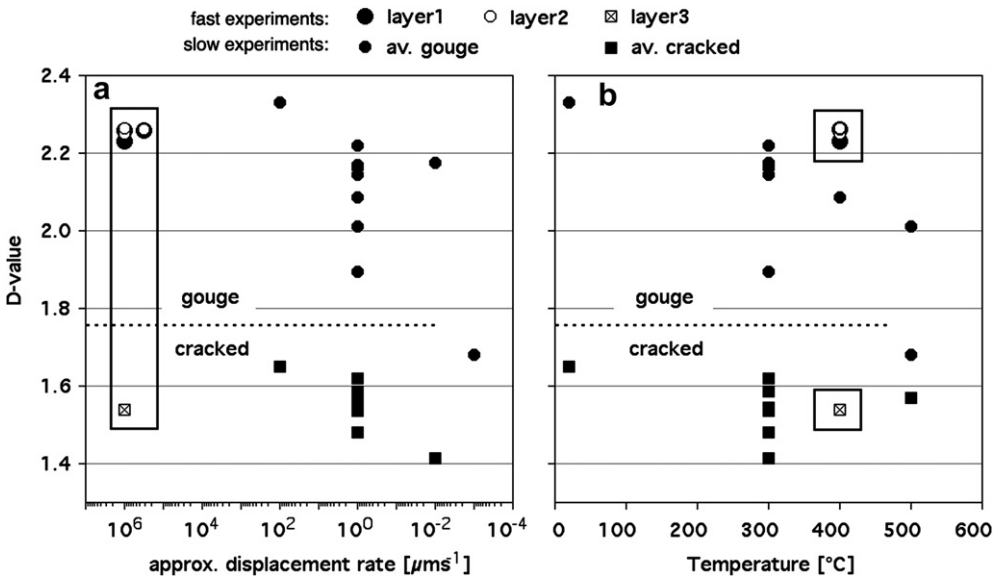

Fig. 7. D-values of the fast slip experiments (framed) in comparison to D-values of samples of slow deformation experiments of the same sample material (from Keulen et al., 2007 and Keulen et al. 2008). For the fast slip experiments, one D-value was determined for each of the layers (layers 1 and 2 correspond to gouge, layer 3 to cracked). For the slow deformation experiments, averaged values (quartz and feldspar) for cracked and gouge are shown. (a) D-values plotted against displacement rate. Displacement rates for slow experiments could not be measured directly. (b) The same D-values plotted against temperature of deformation.

quite small, the total shear strains are higher than those of many friction experiments (Marone and Scholz, 1989, Mair and Marone, 1999, Mair et al., 2002). D-values of $D = 2.6$ after shear strains of $\gamma = 1.5$–2 have been observed previously by Marone and Scholz (1989). In 3-dimensional analysis, values of $D = 2.6$ correspond to $D = 1.6$ of the 2-dimensional analysis employed in this study, so that Marone & Scholz' (1989) data corresponds well to the results of this study for small displacement, i.e. for cracked material. Thus, cracked material from our experiments may be similar to damage zones, whereas gouge material from our experiments may be similar to process or slip zones in natural faults.

The results of the GSD and the shape analysis may be used to infer some aspects of the grain comminution process of the gouge. The grain shape evolution continues towards more equant grains with more rounded boundaries and/or more convex shapes during increasing slip (Fig. 6). This shape evolution indicates continuing spalling or attrition at clast boundaries during slip. The GSD, however, shows stable D-values after small amounts of deformation ($\gamma = 20$) and, therefore, is almost independent of the amount of total slip. Thus, attrition and spalling, which are the likely processes of continuing comminution in the sliding gouge, do not change the $D_>$-value of the already existing gouge. From this argument it follows that spalling does not take place by chipping off larger fragments from the clasts but takes place by crushing producing a range of grain sizes at the clast boundaries. Such a spalling process is observed in the fast slip samples: New fine-grained gouge is formed at the boundaries of larger clasts in the gouge (Fig. 4d). Most of the fragments from attrition and spalling are smaller than 1 μm (Fig. 4d), so that attrition contributes mainly to the fine grain size fraction below r_k. The fact that the new fragments from attrition have a dominant size below r_k causes the $D_>$-values to be unchanged even at large displacements.

Temperature does not appear to affect the D-values of the gouge below ~300 °C (Keulen et al., 2007). The temperature due to shear heating in our fast slip experiments has been inferred to be a maximum of ~400 °C from comparison with other fast slip experiments at the same conditions by Boutareaud et al. (2008). The fact that no melt has been detected also suggests that the temperatures have remained below ~500 °C (e.g., Brantut et al., 2008, Mizoguchi et al., 2007). The temperatures of the fast slip rate experiments are in the same range as the slow deformation experiments, which were carried out at 300 °C and 500 °C.

It is rather difficult to estimate the influence of the microstructural development on the mechanical properties of the gouge. The slip rate has a strong effect on the slip weakening behavior of the experiments (Fig. 2), as is commonly observed in gouge

Table 2
Results of slow experiments performed on a Griggs deformation apparatus. Data from Keulen et al., 2007 and Keulen et al., 2008.

Sample	Temp. of Deform. [°C]	Strain Rate [10^{-4} s^{-1}]	D-values feldspar		D-values quartz		Average D-values	
			Cracked	Gouge	Cracked	Gouge	Cracked	Gouge
12 nk	20	~100[a]					1.65	2.33
38 nk	300	1.5	1.68	2.03	1.56	2.26	1.62	2.14
64 nk	300	1.3	1.52	2.06	1.44	2.26	1.48	2.16
102 nk	300	1.3	1.52	2.07	1.55	2.27	1.53	2.17
60 nk	300	1.5	1.37	1.85	1.72	1.94	1.55	1.89
63 nk	300	1.4	1.62	2.12	1.55	2.32	1.59	2.22
66 nk	300	0.015	1.37	2.09	1.46	2.26	1.41	2.17
91 nk	400	1.3		1.99		2.18		2.09
68 nk	500	1.4	1.67	1.95	1.47	2.07	1.57	2.01
72 nk	500	0.0013	1.68	1.68			1.68	1.68

[a] Strain rate for sample 12 nk is estimated.

experiments (e.g. Marone, 1998, Beeler et al., 1996, Mair and Marone 1999) and in fast slip experiments (e.g., Mizoguchi et al., 2007). As the GSD is not affected by the slip rate at all, weakening of the fault rock cannot depend on the produced GSD of the gouge. As the mechanical properties will depend on the friction of the gouge (Mair and Marone, 1999, Mair et al., 2002, Guo and Morgan, 2004, 2006), the sliding in the existing gouge is more controlled by friction, rolling, and sliding of particles and probably not so much on the comminution process. According to this study, fault gouge which has accommodated small or large amounts of slip appears to have very similar D-values. The D-values in nature all appear to be rather similar and comparable to experimental ones (Wilson et al., 2003, 2005, Monzawa & Otsuki, 2003, Chester et al., 2005, Ma et al., 2006, Sammis and King, 2007, Keulen et al., 2007, 2008). The final D-values of the gouge develop after small displacement (i.e., after a maximum of $\gamma = 20$), so that one parameter which could potentially be affected by the GSD is the slip weakening distance as it may depend on the grain comminution.

4.2. Geological application

One motivation for this study has been to investigate whether information on fault processes (seismic or aseismic) can be extracted from the microstructures of natural fault rocks if the conditions of their deformation are known. The grain size distribution (GSD) is one parameter which is readily quantified in fault rocks (Sammis et al., 1987, Sammis and Biegel, 1989, Marone and Scholz, 1989, Blenkinsop, 1991, An and Sammis, 1994, Shao and Zou, 1996, Monzawa and Otsuki, 2003, Wilson et al., 2003, Hadizadeh and Johnson, 2003, Billi and Storti, 2004, Storti et al., 2003, Chester et al., 2005, Ma et al., 2006, Keulen et al., 2007). However, one of the major results of this study is that the GSD is neither dependent on the amount of slip nor on the slip rate. In other words, there appears to be no microstructural criterion so far by which a fault rock can be clearly inferred to have a seismic or aseismic origin. On the other hand, many pseudotachylite-free fault rocks may have a seismic origin, because seismic and aseismic deformation produce the same GSD and microstructure.

Also, it has been proposed that increasing slip will increase the D-value of fault gouge (Sammis and Biegel, 1989, Hattori and Yamamoto, 1999, Hadizadeh and Johnson, 2003, Sammis and King, 2007, Storti et al., 2003, 2007). The results of slow and fast slip experiments demonstrate that the amount of slip necessary to produce a stable D-value in fault gouge is small ($\gamma \leq 20$), so that, unfortunately, the GSD is not a practical tool to assess slip magnitude in fault zones. Furthermore, there is no dependence of the GSD on normal stress within realistic confining pressures for brittle faults from the experimental data (Keulen et al., 2007), so that no information on the depth of faulting can be obtained from the GSD. In addition, it has to be kept in mind that annealing also resets the GSD in the sense that healed gouge reverts from a size distribution with $D \geq 2.00$ to one of freshly fragmented material with $D = 1.6$ (Keulen et al., 2008).

It is possible, however, that a microstructural measure for the amount of slip may be derived because the fragment shapes (angularity, aspect ratio, convex or concave shapes, etc.) show a dependence on the amount of slip and may record some information on slip magnitude, as already described by Mair & Marone (1999) and Storti et al. (2007). This relationship is rather qualitative at this point but the fast slip experiments demonstrate that the relationship also holds for seismic rates of deformation. These, and other parameters, such as the widening of fault zones with increasing displacement (e.g. Scholz, 1987) are probably more promising criteria to extract information about the conditions of natural fault zone formation.

5. Conclusions

From the results of the fast-speed rotary-shear experiments on granitoid fault gouge and their comparison with slow deformation experiments (carried out in a Griggs apparatus) of the same material the following conclusions can be inferred:

The grain size distribution reaches stable $D_>$-values of 2.0–2.3 (2-D-values) for grain sizes above ~ 1 μm after small amounts of displacement (shear strains of $\gamma = 20$). These values are constant to large displacements of up to 40 m ($\gamma = 15{,}000$–$33{,}000$). For grain sizes below ~ 1 μm, the $D_<$-values are always $= 1$.

The D-values are the same for a wide range of displacement rates, from ~ 1 μm/s to ~ 1.3 m/s, once they have reached stable values above a shear strain of ca. $\gamma = 20$. From these data, it is impossible to distinguish between seismic and aseismic fault zones on the basis of their grain size distribution.

Grain shapes evolve during progressive slip towards more equant shapes with smoother grain boundaries and/or more convex shapes. This result is in accord with previous observations by Storti et al. (2003, 2007) in natural fault zones.

The grain size distribution does not vary with normal stress within a range of ~ 0.5 MPa to 500 MPa. Lower D-values are observed only for high confining pressures of ~ 1 GPa (Keulen et al., 2007).

The granitoid gouge is velocity weakening, and the weakening is less pronounced for a slower slip rate. This result is in accord with fast slip velocity experiments on gouge by Mizoguchi et al. (2007).

The grain comminution process takes place by spalling, where mostly very small grain sizes (less than 1 μm) are formed at the clast boundaries. The size range of these grains is below r_k and the D-values is ~ 1, corresponding to the $D_<$-values of the gouge and leaving the $D_>$-values of the gouge unaffected ($D_> = 2.0$ to 2.3) by further deformation. More work is required to substantiate this aspect.

Acknowledgements

Nynke Keulen has been supported by the Freiwillige Akademische Gesellschaft during the course of this project, Willy Tschudin has prepared the thin sections, and the SEM micrographs were taken with support from the Zentrum of Microscopy of Basel University. Discussions with Toshi Shimamoto have helped to understand some of the topics much better. Very constructive reviews by Jafar Hadizadeh and Anne-Marie Boullier have greatly helped to improve this work.

References

An, L.-J., Sammis, C., 1994. Particle size distribution of cataclastic fault materials from southern California: a 3-D study. Pure & Applied Geophysics 143, 203–227.
Barrett, S.D., 2002. Software for scanning microscopy. Proceedings – Royal Microscopical Society 37, 167–174.
Beeler, N., Tullis, T., Weeks, J., 1996. Frictional behavior of large displacement experimental faults. Journal of Geophysical Research 101, 8697–8715.
Billi, A., Storti, F., 2004. Fractal distributions of particle size in carbonate cataclastic rocks from the core of a regional strike slip fault. Tectonophysics 384, 115–128.
Blenkinsop, T., 1991. Cataclasis and processes of particle size reduction. Pure & Applied Geophysics 136, 60–86.
Boutareaud, S., Calugaru, D.G., Han, R., Fabbri, O., Mizoguchi, K., Tsutsumi, A., Shimamoto, T., 2008. Clay-clast aggregates: A new textural evidence for seismic fault sliding? Geophysical research Letters 35, L05302, doi:10.1029/2007GL032554.
Brantut, N., Schubnel, A., Rouzaud, J.-N., Brunet, F., Shimamoto, T., 2008. High-velocity frictional properties of a clay-bearing fault gouge and implications for earthquake mechanics. Journal of Geophysical Research 113 (B10401). doi:10.1029/2007JB005551.
Chester, J., Chester, F., Kronenberg, A., 2005. Fracture surface energy of the Punchbowl fault, San Andreas system. Nature 437, 133–136.
Cowan, D.S., 1999. Do faults preserve a record of seismic slip? A field geologisťs opinion. Journal of Structural Geology 21, 995–1001.

Guo, Y., Morgan, J.K., 2004. Influence of normal stress and grain shape on granular friction: results of discrete element simulations. Journal of Geophysical Research 109 (B12305). doi:10.1029/2004JB003044.
Guo, Y., Morgan, J.K., 2006. The frictional and microstructural effects of grain comminution in fault gouge from distinct element simulations. J. Geophys. Res. 111 (B12406). doi:10.1029/205JB004049.
Han, R., Shimamoto, T., Ando, J., Ree, J.H., 2007a. Seismic slip record in carbonate-bearing fault zones: an insight from high-velocity friction experiments on siderite gouge. Geology 35, 1131–1134.
Han, R., Shimamoto, T., Hirose, T., Ree, J.H., Ando, J., 2007b. Ultralow friction of carbonate faults caused by thermal decomposition. Science 316, 878–881.
Hattori, I., Yamamoto, H., 1999. Rock fragmentation and particle size in crushed zones of faulting. Journal of Geology 107, 209–222.
Hadizadeh, J., Johnson, W., 2003. Estimating local strain due to comminution in experimental cataclastic textures. Journal of Structural Geology 25, 1973–1979.
Heilbronner, R., Keulen, N., 2006. Grain size and grain shape analysis of fault rocks. Tectonophysics 427 (1–4), 199–216. doi:10.1016/j.tecto.2006.05.020.
Hirose, T., Shimamoto, T., 2003. Fractal dimension of molten surfaces as a possible parameter to infer the slip-weakening distance of faults from natural pseudotachylites. Journal of Structural Geology 25, 1569–1574.
Hirose, T., Shimamoto, T., 2005. Growth of molten zone as a mechanism of slip weakening of simulated faults in gabbro during frictional melting. Journal of Geophysical Research 110 (B05202). doi:10.1029/2004JB003207.
Hirth, G., Tullis, J., 1994. The brittle-plastic transition in experimentally deformed quartz aggregates. Journal of Geophysical Research 99 (B6), 11731–11747.
Keulen, N., Heilbronner, R., Stünitz, H., Boullier, A.-M., Ito, H., 2007. Grain size distributions of fault rocks: a comparison between experimentally and naturally deformed granitoids. Journal of Structural Geology 29 (8), 1282–1300. doi:10.1016/ j.jsg.2007.04.003.
Keulen, N., Stünitz, H., Heilbronner, R., 2008. Healing microstructures of experimental and natural fault gouge. Journal of Geophysical Research. doi:10.1029/2007JB005039.
Ma, K.F., Tanaka, H., Song, S.R., Wang, C.Y., Hung, J.H., Tsai, Y.B., Mori, J., Song, Y.F., Yeh, E.C., Soh, W., Sone, H., Kuo, L.W., Wu, H.Y., 2006. Slip zone and energetics of a large earthquake from the Taiwan Chelungpu-fault Drilling Project. Nature 444, 473–476. doi:10.1038/nature05253.
Mair, K., Marone, C., 1999. Friction of simulated gouge for a wide range of velocities and normal stresses. Journal of Geophysical Research 104, 28899–28914.
Mair, K., Frye, K., Marone, C., 2002. Influence of grain characteristics on the friction of granular shear zones. Journal of Geophysical Research 107 (B10) ECV 4-1; doi:2001JB000516.
Marone, C., 1998. The effect of loading rate on static friction and the rate of fault healing during the earthquake cycle. Nature 391, 69–72.
Marone, C., Scholz, C., 1989. Particle-size distribution and microstructures within simulated gouge. Journal of Structural Geology 11 (7), 799–814.
McKenzie, D., Brune, J.N., 1972. Melting on fault planes during large earthquakes. Geophysical Journal of the Royal Astronomical Society 29, 65–78.
Mizoguchi, K., Hirose, T., Shimamoto, T., Fukuyama, E., 2007. Reconstruction of seismic faulting by high-velocity friction experiments: an example of the 1995 Kobe earthquake. Geophysical Research Letters 34 (L01308). doi:10.1029/2006GL027931.
Monzawa, N., Otsuki, K., 2003. Comminution and fluidization of granular fault materials: implications for fault slip behavior. Tectonophysics 367, 127–143.
Murata, A., Takemura, K., Miyata, T., Lin, A., 2001. Quaternary vertical offset and average slip rate of the Nojima fault on Awaji Island, Japan. The Island Arc 10, 360–367.
Panozzo, R., 1983. Two-dimensional analysis of shape fabric using projections of digitized lines in a plane. Tectonophysics 95, 279–294.
Panozzo, R., 1984. Two-dimensional strain from the orientation of lines in a plane. Journal of Structural Geology 6, 215–221.
Sammis, C., Osborne, R., Anderson, J., Banerdt, M., White, P., 1986. Self-similar cataclasis in the formation of fault gouge. Pure & Applied Geophysics 124 (1–2), 53–78.
Sammis, C., King, G., Biegel, R., 1987. The kinematics of gouge deformation. Pure & Applied Geophysics 125, 777–812.
Sammis, C., Biegel, R., 1989. Fractals, fault-gouge, and friction. Pure & Applied Geophysics 131 (1/2), 255–271.
Sammis, C.G., King, G.C.P., 2007. Mechanical origin of power law scaling in rock. Geophysical Research Letters 34 (L04312). doi:10.1029/2006GL028548.
Scholz, C.H., 1987. Wear and gouge formation in brittle faulting. Geology 15, 493–495.
Shao, S.-M., Zou, J.-C., 1996. Fractal research of fault gouge. Acta Seismologica Sinica 9 (3), 485–491.
Shimamoto, T., Tsutsumi, A., 1994. A new rotary-shear high-velocity frictional testing machine: its basic design and scope of research. Structural Geology 39, 65–78 (in Japanese with English abstract).
Sibson, R.H., 1975. Generation of pseudotachylyte by ancient seismic faulting. Geophysical Journal of the Royal Astronomical Society 43, 775–794.
Sibson, R.H., 1989. Earthquake faulting as a structural process. Journal of Structural Geology 11, 1–14.
Spray, J.G., 1987. Artificial generation of pseudotachylyte using friction welding apparatus: simulation of melting on a fault plane. Journal of Structural Geology 9, 49–60.
Spray, J.G., 1992. A physical basis for the frictional melting of some rock-forming minerals. Tectonophysics 205, 19–34.
Spray, J.G., 1995. Pseudotachylyte controversy: fact or friction? Geology 23, 1119–1122.
Spray, J.G., 1997. Superfaults. Geology 25, 579–582.
Storti, F., Billi, A., Salvini, F., 2003. Particle size distributions in natural carbonate fault rocks; insights for non-self-similar cataclasis. Earth and Planetary Science Letters 206 (1–2), 173.
Storti, F., Balsamo, F., Salvini, F., 2007. Particle shape evolution in natural carbonate granular wear material. Terra Nova 19, 344–352.
Tsutsumi, A., Shimamoto, T., 1994. An attempt to measure the temperature of frictional melts of rocks produced during rapid fault motion. Structural Geology 39, 103–114 (in Japanese with English abstract).
Tsutsumi, A., Shimamoto, T., 1997. High-velocity friction properties of gabbro. Geophysical Research Letters 24, 699–702.
Wilson, J., Chester, J., Chester, F.M., 2003. Microfracture analysis of fault growth and wear processes, Punchbowl fault, San Andreas system, California. Journal of Structural Geology 25 (11), 1855–1873.
Wilson, B., Dewers, T., Reches, Z., Brune, J., 2005. Particle size and energetics of gouge from earthquake rupture zones. Nature 434, 749–752.